

Implementation and testing of wave generation by source distributions in the Globouss model

G. Pedersen

Department of Mathematics, University of Oslo, PO box 1053, 0316 Oslo, Norway

August 6, 2008

Abstract

This report is an extension of an earlier documentation on a Boussinesq solver. It addresses wave generation by submarine slides, or source-sink distributions at the bottom due to other causes. First the implementation is briefly described. A test case, allowing exact solutions both in the discrete and continuous description, is then designed. It is documented that the software implementation reproduces the exact discrete wave generation, within the accuracy of finite arithmetic. Then the performance in a non-exact application is shown.

1 Introduction

For the simulation of tsunamis from earthquakes the vertical uplift of the sea-bed is generally copied onto the surface as an initial condition, sometimes slightly modified to avoid sharp and unphysical gradients [2, 5]. Submarine slides, on the other hand, are much slower processes and wave generation models thus require a source representation of finite extent in time and space. One of the simplest options is to specify a pre-defined sink/source distribution in a long wave model. This enables an approximate description of mass gravity flows that are parameterized or described by separate models.

Herein the implementation of a simple sink/source distribution in the Globouss model is described briefly. The Globouss model is documented in [4] and employed in [6]. The notation and conventions from [4] are generally adopted without further explanation.

2 Time dependent bottom and long wave equations

When only the linear source terms are retained we obtain the standard Boussinesq equations on the form (see, for instance, [7])

$$c_\phi \frac{\partial \eta}{\partial t} = -\nabla \cdot \vec{Q} + c_\phi q, \quad q \equiv -\frac{\partial h}{\partial t}, \quad (1)$$

$$\frac{\partial \vec{v}}{\partial t} + \epsilon \dots = \dots + \mu^2 \dots + \frac{1}{2} \mu^2 h \nabla \frac{\partial^2 h}{\partial t^2}, \quad (2)$$

where \vec{v} is the averaged velocity and \vec{Q} is the flux density. Nonlinear flux terms are given in [3] where also their effects on a benchmark test case are quantified. For higher order modelling of submarine slides in a long wave context see [1]. The source term in the momentum equation is an

order μ^2 smaller than the one in the continuity equation. More important, the triple derivatives will be difficult to represent properly for realistic source distributions. It is likely that whenever the $O(\mu^2)$ source term becomes crucial the whole approach of representing the slide through time dependent bottom is insufficient. Hence, we consider only the leading order source term in the continuity equation.

3 Numerical implementation of a bottom source

The source distribution $q(x, y, t)$ is represented by a sequence of spatial fields $q^{(n)}$, for $n = 1, \dots, N_t$, where n relates to the time. The temporal resolution may be nonuniform, but the fields must be numbered chronologically. Each field, $q^{(n)}$, is discretized on a rectangular grid, $G^{(n)}$ that may be different for each n , but that must be specified in the same coordinate system as the depth matrix. The source field is then extended to the whole x, y plane by setting $q^{(n)}$ to zero outside $G^{(n)}$ and by interpolation withing $G^{(n)}$. The interpolation is based on either bi-linear polynomials, which is generally recommended, or bi-quadratic splines, that should be used only with great care.

For the temporal integration of q two methods suggest themselves, namely treating q as piecewise constant or piecewise linear. The latter seems to be more efficient, but the former yields a simpler implementation (in particular when the $G^{(n)}$ depend on n). In addition, when the piecewise constant value is specified at the centre of integration intervals the piecewise constant representation yields an equally accurate integral. Even though this may not be entirely true when the integral is invoked in the wave equations we select the piecewise constant representation. A set of times T_0, \dots, T_{N_t} is then defined and $q^{(n)}$ is interpreted as the source distribution acting in the time interval $[T_{n-1}, T_n]$. For t outside the interval $[T_0, T_{N_t}]$ the q is put to zero. Of course, several sources, with no temporal overlap, may be included by intervening intervals with zero sources.

The discrete continuity equation now becomes

$$[\delta_t \eta = -r_y(\dots) + \frac{1}{\Delta t} < q >]_{i+\frac{1}{2}, j+\frac{1}{2}}^{(k+\frac{1}{2})} \quad (3)$$

If we assume that $k\Delta t$ and $(k+1)\Delta t$ are located in the intervals $[T_{n_a-1}, T_{n_a}]$ and $[T_{n_b-1}, T_{n_b}]$, respectively, the integrated flux is given by

$$\begin{aligned} [< q >]_{i+\frac{1}{2}, j+\frac{1}{2}}^{(k+\frac{1}{2})} &= (T_{n_a} - k\Delta t)q^{(n_a)} + \sum_{p=n_a+1}^{n_b-1} (T_p - T_{p-1})q^{(p)} + ((k+1)\Delta t - T_{n_b})q^{(n_b)} \\ &\approx \int_{k\Delta t}^{(k+1)\Delta t} q dt, \end{aligned} \quad (4)$$

where the interpolated values corresponding to the correct spatial position is used on the right hand side. Naturally, only one, or two, of the right hand terms in the first line of (4) may contribute, according to the temporal resolutions. The sources may also be incorporated in h .

4 A simple sink/source distribution

A test case is designed by an inverse approach. We neglect all terms of order ϵ, μ^2 , the variation of the map factors, and the changes in h due to the bottom fluxes. Then we decide on a solution

of the form

$$\eta = tF(x, y), \quad \vec{v}(x, y, 0) = 0, \quad (5)$$

where F is a given function. From (1) and (2) it now follows

$$F = -\nabla \cdot (h\vec{v}) + q,$$

$$\frac{\partial \vec{v}}{\partial t} = -t\nabla F.$$

With the initial condition in (5) this set is readily solved for \vec{v} and q

$$\vec{v} = -\frac{1}{2}t^2\nabla F(x, y), \quad q = F - \frac{1}{2}t^2\nabla(h\nabla F). \quad (6)$$

Of course there is hardly any interesting physical case represented by this source distribution. However, that is completely irrelevant since the solution will be used only for program assessment.

In the numerical realisation we choose the shape function

$$F(x, y) = F_0 e^{-\{k(x-\hat{x})\}^2 - \{\ell(y-\hat{y})\}^2}. \quad (7)$$

This is discretized on a rectangular domain with $(\hat{x} - \frac{1}{2}L, \hat{y} - \frac{1}{2}B)$ and $(\hat{x} + \frac{1}{2}L, \hat{y} + \frac{1}{2}B)$ as lower left and upper right corner, respectively. For q we employ a uniform resolution, in both space and time, that may, or may not, coincide with the grid used in the wave computations. The formulae in (6) may either be used directly or replaced by their discrete counterparts, such as in the next section.

5 An exact discrete test

For simplicity we assume constant depth, $h = h_0$, and grids $G^{(n)}$ (independent of n) with nodes that coincide with those of η . The values of q are specified at the same times as \vec{v} and hence renumbered with semi-integral superscripts. The discrete source field is then defined according to

$$[q = F - \frac{1}{2}h_0t^2(\delta_x^2 + \delta_y^2)F]_{i+\frac{1}{2},j+\frac{1}{2}}^{(k+\frac{1}{2})}, \quad (8)$$

where F is discretized on the same spatial grid as q and η and we employ the identity

$$t^{(\alpha)} \equiv \alpha\Delta t,$$

in this and subsequent expressions. The source strength $q^{(k+\frac{1}{2})}$ then applies to the time period $[t^{(k)}, t^{(k+1)}] = [k\Delta t, (k+1)\Delta t]$ and we obtain simply

$$[< q > = \Delta t q]_{i+\frac{1}{2},j+\frac{1}{2}}^{(k+\frac{1}{2})}.$$

Correspondingly the solutions for η , u and v are written

$$[\eta = tF]_{i+\frac{1}{2},j+\frac{1}{2}}^{(k)},$$

$$[u = -\frac{1}{2}t^2\delta_x F]_{i,j+\frac{1}{2}}^{(k+\frac{1}{2})}, \quad [v = -\frac{1}{2}t^2\delta_y F]_{i+\frac{1}{2},j}^{(k+\frac{1}{2})}. \quad (9)$$

A centred first order difference will reproduce the derivative exactly for polynomials of degree two or lower (see error analysis in [4]). Hence, the expressions in (8) and (9) will fulfil the discrete equation set

$$[\eta = -h_0(\delta_x u + \delta_y v) + q]_{i+\frac{1}{2}, j+\frac{1}{2}}^{(k+\frac{1}{2})}, \quad (10)$$

$$[\delta_t u = -\delta_x \eta]_{i, j+\frac{1}{2}}^{(k)}, \quad [v = -\delta_y \eta]_{i+\frac{1}{2}, j}^{(k)}. \quad (11)$$

To reproduce (9) exactly (except for finite precision errors) in a Globouss simulation we must provide also the initial conditions

$$[u^{(i)} = -\frac{1}{8}\Delta t^2 \delta_x F]_{i, j+\frac{1}{2}}, \quad [v^{(i)} = -\frac{1}{8}\Delta t^2 \delta_y F]_{i+\frac{1}{2}, j}.$$

Since the initial surface elevation is zero the initial velocities will be reproduced by the velocities at both $-\frac{1}{2}\Delta t$ and $\frac{1}{2}\Delta t$.

5.1 The simulation

For these simulations the compilation of Globouss is made by gfortran (GNU Fortran 4.2.1) with either 32 bit or 64 bit floating numbers. The parameters were

$$h_0 = 1.0, \quad F_0 = 0.7, \quad k = 0.04, \quad \ell = 0.035, \quad L = 60, \quad B = 120, \quad \Delta x = 0.75, \quad \Delta y = 1.5, \\ \Delta t = 0.07, \quad \hat{x} = 0, \quad \hat{y} = 30, \quad x_0 = -29.625, \quad y_0 = -29.25, \quad n = 79, \quad m = 79.$$

The maximum simulation time is $t_m = 0.7$. As seen from the table the computational domain is larger than the source region, but the grids are still coinciding. The extreme deviations in η after t_m became

| precision | min. dev. | max. dev. |
|-----------|------------------------------------|----------------------------------|
| 32 bit | $-2.9802322 \cdot 10^{-8}$ | $2.9802322 \cdot 10^{-8}$ |
| 64 bit | $-4.44089209850063 \cdot 10^{-15}$ | $7.5245432243869 \cdot 10^{-15}$ |

The deviations are clearly consistent with the action of errors due to finite arithmetic only.

6 Grid refinement test

Parameter values defining the source and depth are now selected as

$$h_0 = 1.0, \quad F_0 = 0.7, \quad k = 0.04, \quad \ell = 0.035, \quad L = 40, \quad B = 40, \quad t_m = 0.7.$$

Grids are no longer exactly coinciding in space or time and the formula for q in (6) is used for the source instead of the discrete counterpart. For both the velocities and the surface elevation we use zero as initial condition and the simulations are run in 32 bit mode. Bi-linear interpolation are used in space. When the spatial (equal in both directions) and temporal increments in the source is defined as Δs and Δt_s , respectively, a sequence of refinements then yields

| resolution | min. dev. | max. dev. |
|--|----------------------|---------------------|
| $\Delta s = 1.67, \Delta t_s = 0.14, \Delta x = 2.5, \Delta y = 2.08, \Delta t = 0.058$ | $-1.8 \cdot 10^{-2}$ | $2.8 \cdot 10^{-3}$ |
| $\Delta s = 0.816, \Delta t_s = 0.07, \Delta x = 1.22, \Delta y = 1.02, \Delta t = 0.058$ | $-5.6 \cdot 10^{-3}$ | $9.4 \cdot 10^{-4}$ |
| $\Delta s = 0.404, \Delta t_s = 0.035, \Delta x = 0.606, \Delta y = 0.505, \Delta t = 0.058$ | $-1.1 \cdot 10^{-3}$ | $1.8 \cdot 10^{-4}$ |

The results corresponding to the last line is shown in figure 1. The largest deviations are found in the middle of the source region, but small errors are also observed as outwardly propagating waves.

7 Finishing remarks

A robust and general implementation of bottom sources is described. It is validated through the reproduction of an exact discrete solution. In this case no interpolation takes place since the grids of the source and the simulation are commensurable. Moreover, for a particular source, designed for control and simplicity, the interpolation parts of the algorithm are tested and shown to yield decreasing errors with increased resolution. However, two tasks remain before the source facility may be put into proper use

1. Pre-processing tools must be created to produce the input in the required format. These tools will depend on the application.
2. The algorithm should be put to test in application of realistic slides, including grid refinement and parameter sensitivity.

References

- [1] P. J. Lynett and P. L.-F. Liu. A numerical study of submarine-landslide-generated waves and run-up. *Proceedings of The Royal Society: Mathematical, Physical and Engineering Sciences*, 458(2028):2885–2910, 2002.
- [2] G. Pedersen. A note on tsunami generation by earthquakes. Preprint Series in Applied Mathematics 4, Dept. of Mathematics, University of Oslo, Norway, 2001.
- [3] G. Pedersen. Modeling run-up with depth integrated equation models. In P. L.-F. Liu, H. Yeh, and C. E. Synolakis, editors, *Advanced Numerical Models for Simulating Tsunami Waves and Runup edited*, volume 10 of *Advances in Coastal and Ocean Engineering*. World Scientific Publishing, 2008.
- [4] G. Pedersen and F. Løvholt. Documentation of a global Boussinesq solver. Preprint Series in Applied Mathematics 1, Dept. of Mathematics, University of Oslo, Norway, 2008. **URL:** http://www.math.uio.no/eprint/appl_math/2008/01-08.html.
- [5] F. Løvholt, H. Bungum, C.B. Harbitz, S. Glimsdal, C. D. Lindholm, and G. Pedersen. Earthquake related tsunami hazard along the western coast of Thailand. *Natural hazards and earth system sciences*, 6:1–18, 2006.
- [6] F. Løvholt, G. Pedersen, and G. Gisler. Oceanic propagation of a potential tsunami from the la palma island. *J. Geophys. Res.*, In press(X):xxx, 2008. DOI:10.1029.
- [7] T. Y. Wu. Long waves in ocean and coastal waters. *Proc. ASCE, J. Eng. Mech. Div.*, 107:501–522, 1981.

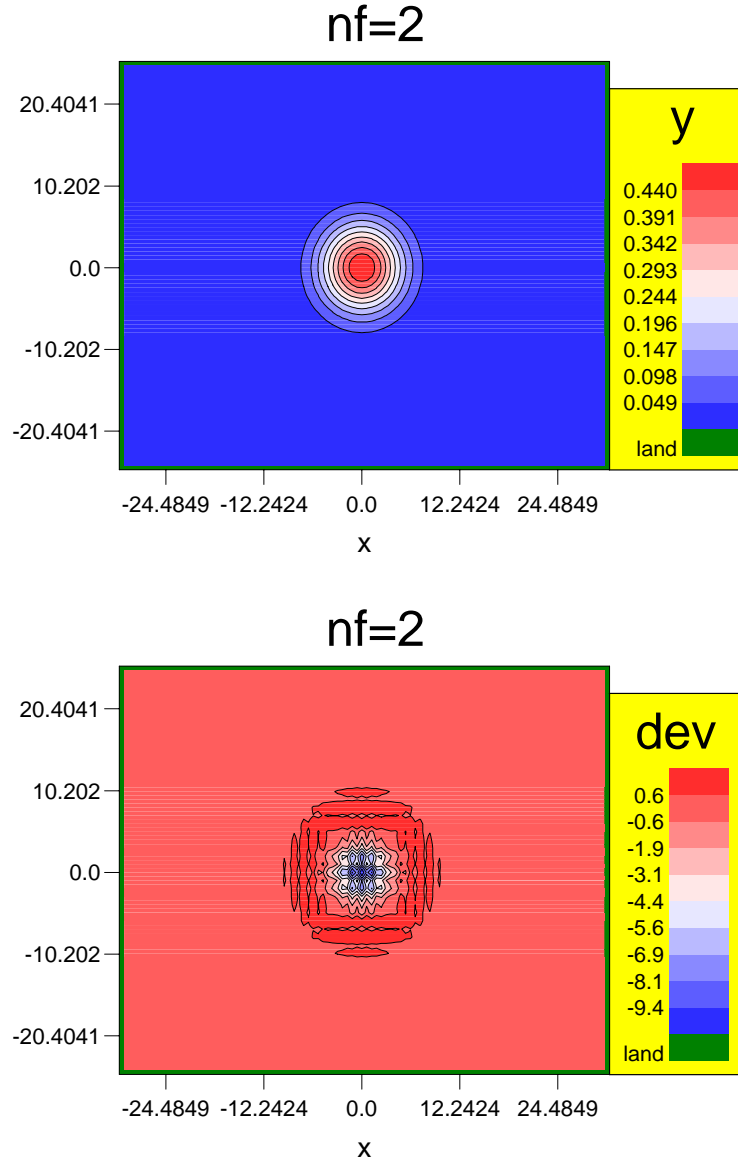


Figure 1: Simulation with $\Delta s = 0.404$, $\Delta t_s = 0.035$, $\Delta x = 0.606$, $\Delta y = 0.505$, $\Delta t = 0.058$. Left panel: the computed surface elevation. Right panel: the deviation from the exact value times 10^4 .